


Intermittent trapping of spiral waves in a cardiac modelWouter-Jan Rappel ^{*}*Department of Physics, University of California, San Diego, California 92093, USA*

(Received 12 October 2021; accepted 21 December 2021; published 5 January 2022)

Spiral waves are found in many excitable systems and are thought to play a role in the incoherent electrical activation that underlies cardiac arrhythmias. It is well-known that spiral waves can be permanently trapped by local heterogeneities. In this paper, we demonstrate that spiral waves can also be intermittently trapped by such heterogeneities. Using simulations of a cardiac model in two dimensions, we show that a tissue heterogeneity of sufficient strength or size can result in a spiral wave that is trapped for a few rotations, after which it dislodges and meanders away from the heterogeneity. We also show that these results can be captured by a particle model in which the particle represents the spiral wave tip. For both models, we construct a phase diagram which quantifies which parameter combinations of heterogeneity size and strength result in permanent, intermittent, or no trapping. Our results are consistent with clinical observations in patients with atrial fibrillation that showed that spiral wave reentry can be intermittent.

DOI: [10.1103/PhysRevE.105.014404](https://doi.org/10.1103/PhysRevE.105.014404)**I. INTRODUCTION**

Spiral waves are a common feature in excitable media and have been observed in several chemical systems, including the Belousov-Zhabotinsky reaction system [1,2] and surface catalytic oxidation reaction systems [3]. They are also common in biological systems, for example, in the form of waves of chemoattractants during the aggregation process of *Dicystostelium discoideum* cells [4] and as waves of depolarization in chicken retinas [5], where they have been associated with the progression of macular degeneration [6]. Spiral waves also play a major role in cardiac arrhythmias [7]. Specifically, they are believed to underlie fibrillation, during which organized electrical activity is disrupted and replaced by wave propagation that is fast and irregular and compromises the primary mechanical function of the heart. When occurring in the ventricles, fibrillation is lethal within minutes [8], while atrial fibrillation (AF), the most common arrhythmia in the U.S. [9], results in an elevated risk for stroke and increased morbidity and mortality [10,11].

Modeling studies using homogeneous domains, i.e., domains where all model parameters are the same, have shown that a single spiral wave can destabilize through a variety of mechanisms [12]. When the electrical wave of the spiral locally breaks, it results in waves that reenter previously excited tissue, thus forming new spiral waves. The resulting dynamical state can be classified as spiral defect chaos, with a stochastically fluctuating number of spiral waves and spiral wave tips that meander through the domain [13–15]. Reentry in homogeneous domains or tissue is classified as functional [16] and can be contrasted with anatomical reentry, during which a spiral wave rotates around a tissue heterogeneity. In models, these heterogeneities can be easily introduced by modifying one of the model parameters, while in ac-

tual tissue these heterogeneities can take on the form of anatomical obstacles or fibrotic scar [17,18]. A number of numerical studies have investigated the conditions for the anchoring of spiral waves to heterogeneities [19–25], while the permanent trapping of reentry waves to obstacles has also been demonstrated in *in vitro* and in *in vivo* experiments [26,27].

Although anchoring of spiral waves to obstacles has been well studied in numerical models, it is less clear if spiral waves can also attach *intermittently* to heterogeneities. In this case, a spiral wave would meander through the tissue and would be trapped to a heterogeneity for several rotations, after which it would dislodge again. This question is relevant since *in vitro* experiments have demonstrated that spiral waves can pin and unpin from obstacles [27]. Moreover, results from clinical work suggest that intermittent spiral wave trapping may play a role in AF [28–30]. More precisely, these clinical studies have found that spiral waves in humans can appear intermittently in certain regions of the heart and that their tips can migrate over considerable distances.

In this paper, we used simulations of a cardiac model to investigate the dynamics of a spiral wave in the presence of a circular heterogeneity of variable sizes, modeled by reducing the local excitability. We show that, depending on the size and strength of the heterogeneity, the spiral wave is either permanently, intermittently, or not trapped at all. Furthermore, by computing a phase diagram, we show that a minimum size and strength is required for intermittent trapping. We also show that this qualitative behavior can be captured by a particle model, representing the dynamics of the spiral wave tip. In this model, the particle moves under the influence of two forces, resulting in a tip trajectory that is consistent with the full, spatially extended model, and a potential well, representing the heterogeneity. As is the case for the full model, we constructed a phase diagram and showed that intermittent trapping is only possible for heterogeneities of intermediate size and strength. Our results suggest that the heterogeneities of medium size

^{*}rappel@physics.ucsd.edu

and strength may be responsible for the clinically observed intermittency during AF.

II. RESULTS

A. 3D simulations

In a first simulation and acting as a motivation for further investigation, we explored wave propagation in a clinically derived geometry of the left atrium. In this simulation and following previous literature (see, e.g., Ref. [7]), the potential u of cardiac cells is described as

$$\frac{\partial u}{\partial t} = D\nabla^2 u - \frac{I_{\text{ion}}}{C_m}. \quad (1)$$

Here, C_m is the capacitance of the membrane, D is a diffusion coefficient, responsible for the spreading of the activation front, and I_{ion} represents membrane currents. In this paper, we chose to model the membrane currents using the Fenton-Karma (FK) model [31], a simple model with only three currents: $I_{\text{ion}} = J_{\text{fi}}(u, v) + J_{\text{so}}(u) + J_{\text{si}}(u, w)$. There, currents are written as

$$J_{\text{fi}}(u, v) = -\frac{v}{\tau_d} \Theta(u - u_c)(1 - u)(u - u_c), \quad (2)$$

$$J_{\text{so}}(u) = \frac{u}{\tau_o} \Theta(u_c - u) + \frac{1}{\tau_r} \Theta(u - u_c), \quad (3)$$

$$J_{\text{si}}(u, w) = -\frac{w}{2\tau_{\text{si}}} (1 + \tanh[k(u - u_c^{\text{si}})]), \quad (4)$$

where Θ is the standard Heavyside function. The gating variables v and w are given by

$$\frac{\partial v}{\partial t} = \Theta(u_c - u)(1 - v)/\tau_v^-(u) - \Theta(u - u_c)v/\tau_v^+,$$

$$\frac{\partial w}{\partial t} = \Theta(u_c - u)(1 - w)/\tau_w^- - \Theta(u - u_c)w/\tau_w^+,$$

where $\tau_v^-(u) = \Theta(u - u_v)\tau_{v1}^- + \Theta(u_v - u)\tau_{v2}^-$ [31]. This model has been extensively used in cardiac modeling literature and its parameters can be adjusted and fitted to different electrophysiological data, including human [12,32]. The parameter values used in this paper are detailed in Table I.

The atrial shell was constructed using patient data using three-dimensional electroanatomic imaging (NavX, St. Jude Medical, Sylmar, CA) [33]. The shell was rendered into a triangular mesh with 39749 nodes and an average internode distance of 0.04 cm. The electrophysiological model was then simulated using a finite volume algorithm fully described in Ref. [34]. As a temporal discretization, we used $\Delta t = 0.0015$ ms, well below the critical discretization for which the simulation became unstable ($\Delta t = 0.005$ ms). Within this atrial geometry, we included a circular region of depressed excitability, modeled by increasing one of the model parameters, τ_d . As an initial condition, we projected a spiral wave obtained using a 2D simulation onto the shell and varied the size of the heterogeneity and the degree of excitability depression. We found that for certain combinations of these parameters, the spiral wave was *intermittently* trapped by the heterogeneity. Increasing the size or depressing the excitability further was found to result in permanently trapped spiral waves while decreasing the size or depressing the excitability less was observed to lead to spiral waves that were not trapped at all. An

TABLE I. Parameters used for the Fenton-Karma model simulations. All time constants τ are in milliseconds, all voltages are in rescaled, arbitrary units, k is dimensionless, D is in units of cm^2/ms , and C_m in units of $\mu\text{F}/\text{cm}^2$.

Parameter	Value
τ_v^+	3.33
τ_{v1}^-	19.6
τ_{v2}^-	1000
τ_w^+	50
τ_w^-	11
$\tau_{d,0}$	0.39
τ_o	8.3
τ_r	50
τ_{si}	45
k	10
u_c^{si}	0.85
u_c	0.13
u_v	0.055
D	0.001
C_m	1

example of a simulation that resulted in intermittent trapping is shown in Fig. 1(a), where we visualized the heterogeneity with a radius of $R_{\text{hetero}} = 0.3$ cm as an orange patch, the membrane voltage using a color code with red (blue) corresponding to depolarized (repolarized) tissue, and the path of the spiral wave tip using gray symbols. In this case, the model parameter was increased from a baseline value of $\tau_{d,0} = 0.39$ ms to $\tau_d = 0.42$ ms.

To further visualize the trapping event, we plotted the distance between the spiral wave tip and the center of the heterogeneity, r , as a function of time in Fig. 1(b). This plot shows that the spiral wave tip moves freely and remote from the heterogeneity before it is captured at $t \approx 2.2$ s. It subsequently rotates around the heterogeneity for several rotations, after which it dislodges and moves away. This sequence is then repeated, resulting in another transient trapping event. In this figure, the time in which the tip is trapped by the hetero-

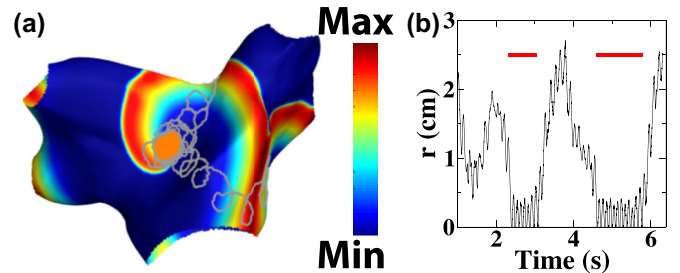


FIG. 1. (a) Snapshot of a computer simulation of the FK cardiac model in a patient-derived left-atrial geometry. The potential is shown using a color scale with red (blue) corresponding to depolarized (repolarized) tissue. The circular heterogeneity (with radius $R_{\text{hetero}} = 0.3$ cm) is shown as an orange patch and the trajectory of the spiral wave tip is plotted in gray. (b) Distance from the heterogeneity as a function of time during trapping events, indicated by the red bars.

generality is indicated by red bars. Thus, this sample simulation shows that for certain parameter values, the introduction of a heterogeneity can intermittently trap a spiral wave.

B. 2D simulations

To systematically determine for which parameters a spiral wave can be intermittently trapped, independent of a patient-specific geometry, we next simulated the model on an isotropic 200×200 square grid with no-flux boundary conditions. We verified that the qualitative behavior is unchanged when using larger domains (300×300 and 400×400), indicating that it is independent of computational boundaries. Simulations were carried out with a spatial discretization of $\Delta x = 0.025$ cm and a temporal discretization of $\Delta t = 0.05$ ms. The equations were solved using the forward Euler scheme and a five-point spatial stencil. As in the 3D sample simulation, we introduced a circular heterogeneity, placed in the middle of the computational domain. As parameters that specify the heterogeneity, we used its radius R_{hetero} and the deviation of τ_d from its baseline value: $\Delta\tau_d \equiv \tau_d - \tau_{d,0}$. We varied R_{hetero} from 0.25 to 3.75 cm in steps of 0.25 cm and $\Delta\tau_d$ from 0.01 ms^{-1} to 0.26 ms^{-1} in steps of 0.01 ms^{-1} . Increasing $\Delta\tau_d$ to even larger values did not change the outcome of the simulations any more. As an initial condition, the simulation was started with a spiral wave, obtained using cross-field stimulations [35], present in the computational domain. In the absence of a heterogeneity and for the parameters chosen in this paper, the spiral wave meanders through the domain.

In Figs. 2(a)–2(c), we show a sequence of three snapshots of a typical simulation in which a spiral wave is intermittently trapped. The tissue potential is represented by gray scale, with white corresponding to fully depolarized and black to fully repolarized tissue, while the location of the heterogeneity is indicated as a dashed white line. The spiral wave tip shows as a cyan dot and the trajectory of the spiral wave during the entire interval captured by the three snapshots is shown in red. The spiral wave tip is initially distant from the heterogeneity [Fig. 2(a)], meanders through the domain, and, when it encounters the heterogeneity, is trapped for several rotations [Fig. 2(b)]. The trapping is not permanent, however, and the spiral wave eventually dislodges and meanders away from the heterogeneity [Fig. 2(c)]. As in the 3D simulation, the trapping of the spiral wave can also be visualized by plotting the distance from the tip to the center of the heterogeneity, r , as a function of time. This is demonstrated in Fig. 2(d), which shows that during three intervals, indicated by the red bars, the spiral wave is trapped. In between these intervals, however, the spiral tip is moving away from the heterogeneity and meanders through the domain.

Our simulations revealed that a spiral wave is either permanently trapped, not trapped at all, or intermittently trapped by the heterogeneity. This is demonstrated in the phase diagram in the $R_{\text{hetero}}-\Delta\tau_d$ space, presented in Fig. 2(e). This phase diagram was constructed by running a simulation with a duration of 50 s for each parameter combination. A trapping event was identified when the spiral wave tip was located within a distance of $3R_{\text{hetero}}$ from the center of the heterogeneity and rotated twice or more around this heterogeneity. A spiral tip that exhibited at least two trapping events during the simu-

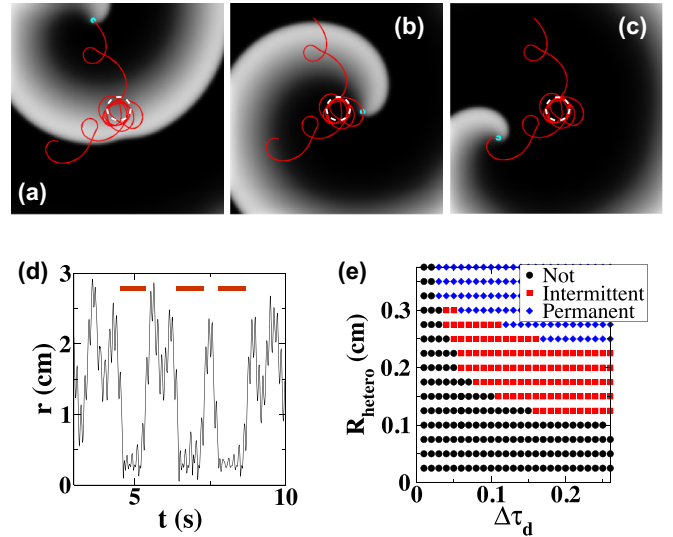


FIG. 2. Results of computer simulations in a square domain with no-flux boundary conditions. (a)–(c) Snapshots of a simulation of a spiral wave just before (a), during (b), and after (c) an intermittent trapping event. The spiral wave tip is shown in red and the potential is plotted using a gray scale. The circular heterogeneity is indicated by the white dashed line. Parameter values: $R_{\text{hetero}} = 0.275$ cm and $\Delta\tau_d = 0.08$ ms^{-1} . (d) The distance of the spiral wave tip to the center of the heterogeneity as a function of time. The intervals during which the tip is trapped in the heterogeneous zone is indicated by the red bars. (e) Phase diagram, indicating for which parameter combination the spiral wave tip is permanently trapped (blue diamonds), intermittently trapped (red squares), or not trapped at all (black circles).

lation was classified as intermittently trapped. In the phase diagram, we have plotted all parameter combinations that did not result in trapping as black circles, all combinations that resulted in permanent trapping as blue diamonds, and those that produced intermittent trapping as red squares. As can be seen from this phase diagram, intermittent trapping was possible for a wide range of sizes and heterogeneity strengths. Furthermore, the phase diagram revealed that both a minimum value of R_{hetero} and a minimum value for $\Delta\tau_d$ are required for intermittent trapping. In addition, once R_{hetero} becomes larger than a second critical value, the spiral wave is trapped indefinitely.

C. Particle model simulations

To further investigate the dynamics of the spiral wave in the presence of a heterogeneity, we turned to a particle model, which only simulates the spiral tip and ignores the spatial extent of the spiral wave. Such an approach was already successfully employed when describing the interaction of a spiral wave with multiple, small-scale heterogeneities [36]. In this approach, the spiral wave tip is modeled as a forced-driven particle moving in a potential. Specifically, the x and y coordinates of the particle (tip) are described by the following equations:

$$\frac{d^2x(t)}{dt^2} = F_1 \cos(\omega_1 t) + F_2 \cos(\omega_2 t) - \xi \frac{dx}{dt} - \frac{dU(x, y)}{dx}, \quad (5)$$

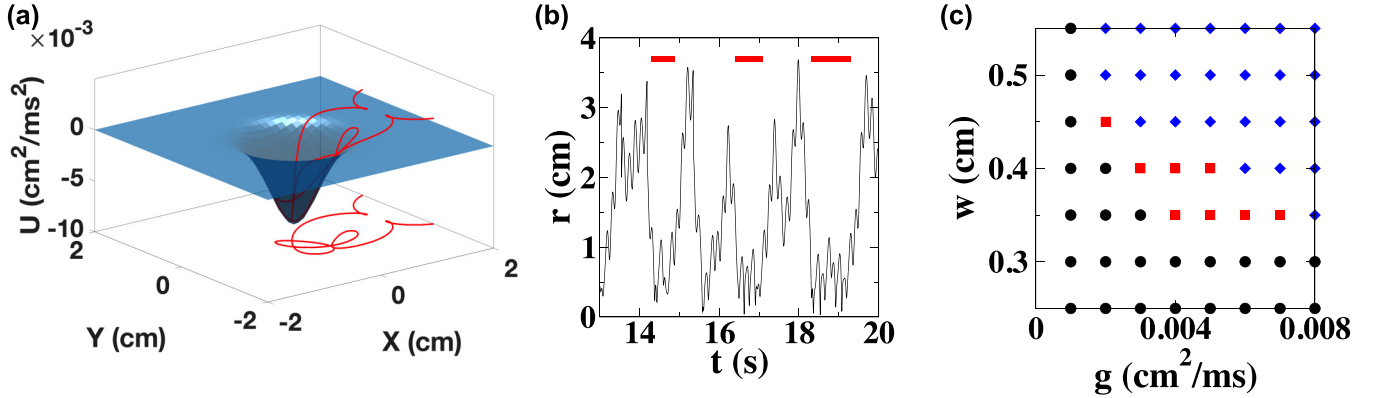


FIG. 3. Results from the particle model. (a) Trajectory of an intermittently trapped particle, moving in a potential surface of depth $g = 0.004 \text{ cm}^2/\text{ms}^4$ and width $w = 0.4 \text{ cm}$. (b) Distance of the particle to the minimum of the potential well, r , as a function of time for identical parameter values. The intervals during which the particle is trapped are indicated using the red bars. (c) Phase diagram, showing the different possible outcomes in the particle models. As in Fig. 2, blue diamonds represent tips that are permanently trapped, red squares correspond to tips that are intermittently trapped, and black circles represent tips that are not trapped.

$$\frac{d^2y(t)}{dt^2} = F_1 \sin(\omega_1 t) + F_2 \sin(\omega_2 t) - \xi \frac{dy}{dt} - \frac{dU(x, y)}{dy}, \quad (6)$$

where the first terms represent a forcing with frequencies ω_1 and ω_2 and amplitudes F_1 and F_2 . As we have shown in our previous study, the parameters of these forces can be quantitatively determined such that the trajectory in the particle model can faithfully reproduce the trajectory in the full, spatially extended model [36]. In our case, the values of these parameters were found to be $\omega_1 = 3.76 \times 10^{-4} \text{ ms}^{-1}$, $\omega_2 = 4.59 \times 10^{-2} \text{ ms}^{-1}$, $F_1 = 3.55 \times 10^{-4} \text{ cm/ms}^2$, and $F_2 = 9.92 \times 10^{-4} \text{ cm/ms}^2$. The third term corresponds to a damping with strength ξ that prevents the model from drifting while the last term describes a potential energy, representing the presence of a heterogeneity.

To mimic heterogeneities, we chose a potential energy term with circular symmetry and a minimum at the location of the heterogeneity [36]. Specifically, we introduced a potential in which the heterogeneity was described by a Gaussian well centered at $x = 0$ and $y = 0$:

$$U(x, y) = -\frac{g}{\sqrt{2\pi}} \left(\exp \left[-\frac{(x^2 + y^2)}{2w^2} \right] \right). \quad (7)$$

In this description, the strength of the heterogeneity is parameterized by the depth of the potential well, g , and its size by the width, w .

For specific values of g and w , we found that the particle was intermittently trapped by the potential well. This is demonstrated in Fig. 3(a), where we show the trajectory of the particle during a trapping event, along with the potential. This is further shown in Fig. 3(b), where we plot, as a function of time, the distance of the particle to the center of the potential well, r . For the plotted interval, the particle is trapped during three intermittent intervals, as indicated by the red bars.

Further comparing the full 2D simulations to the particle model, we next determined the parameter combinations for which the particle is permanently, intermittently, or not trapped in the potential well. We ran simulations for 50 s

and a particle was considered trapped if the distance of its trajectory to the minimum of the potential was smaller than three times the width of the potential (i.e., $3w$) for at least two consecutive rotations. Furthermore, a particle was considered to be intermittently trapped if at least two trapping events occurred within the simulation interval. The results are plotted in Fig. 3(c), where we used the same color and symbol convention as in Fig. 2. As was the case for the 2D simulations (cf. Fig. 2), there exists a region in parameter space for which the particle was intermittently trapped by the potential. For these parameter values, the particle trajectory entered the potential well and was rotated several times within this well, after which it escaped from the well. Also as in the 2D case, this intermittent trapping required both a minimal heterogeneity size as well as a minimal potential well depth.

III. SUMMARY AND DISCUSSION

To summarize, we demonstrated for certain parameter values in a spatially extended cardiac model, a spiral wave tip can be intermittently trapped by a tissue heterogeneity. During these intermittent trapping events, the spiral wave tip circles around the heterogeneity for a variable amount of time but eventually becomes dislodged and moves away from the heterogeneity. After meandering through the domain, the tip is then again trapped at the heterogeneity for a brief period, after which the sequence repeats itself. In our simulations, the heterogeneity was introduced by varying one of the model parameters that parametrized tissue excitability. We should note, however, that we have verified that changing other parameters in the full model can also result in intermittent trapping, introducing a region of reduced values of the diffusion constant D .

Using simulations, we obtained a phase diagram, which quantifies for which parameter values the spiral wave can be intermittently trapped. This phase diagram revealed that intermittent trapping requires a minimum size of the heterogeneity. This is expected since for these very small sizes, the front of an attached spiral wave will encounter the back of the wave, resulting in detachment and no trapping. The phase diagram also showed that above a certain size, the

spiral wave is permanently trapped. This is consistent with experimental and computational work, which demonstrated that the tip of a spiral wave can become permanently attached to heterogeneities that are larger than a certain minimum size [19,37]. Thus, intermittent trapping is only possible for intermediate heterogeneity sizes. For these sizes, when the meandering spiral wave encounters the heterogeneity, it can be captured, resulting in the tip rotating around the heterogeneity. However, the distance of the spiral tip to the center of the heterogeneity slowly increases with each rotation [see Fig. 2(d)]. When this distance becomes too large, the spiral wave detaches from the heterogeneity and meanders away from it. When the spiral tip encounters the heterogeneity again, this scenario can be repeated, resulting in intermittent trapping. The phase diagram also showed that intermittent trapping requires a minimal strength of the heterogeneity, parameterized here by the deviation of the excitability parameter τ_d from its baseline value, $\Delta\tau_d$. This can be intuitively understood by realizing that for very small values of $\Delta\tau_d$ the change in excitability will have a minimal effect on the propagation of the spiral wave.

The intermittent trapping observed in the full model can be recapitulated in a simple model in which the reaction-diffusion system is replaced by a set of equations that describe the x and y coordinates of a particle moving in a potential well and subject to two forces. We have shown that, for certain parameter values of the potential, the particle can also be intermittently trapped, consistent with the full model. Thus, the particle model can accurately describe the qualitative dynamics of the full model, with the depth of the potential well parametrizing the strength of the heterogeneity and its spatial extent playing the role of the heterogeneity size. This suggests that the trapping in the full model is due to the presence of an effective potential well at the location of the heterogeneity.

For the particle model, we also obtained a phase diagram, which quantifies for which parameter values the spiral wave can be intermittently trapped. As for the full model, the phase diagram showed that intermittent trapping only occurs for intermediate sizes of the potential well. This can be seen by considering a fixed strength of the heterogeneity, in this case the depth of the potential well, and varying the size of the potential well. As expected, for small sizes, the spiral wave was not affected by the presence of the potential well. Furthermore, and consistent with the full model, for large sizes the particle was permanently trapped.

A similar argument can be made when considering a fixed value of the potential well size and varying the strength of the heterogeneity. Again, as expected, for weak heterogeneities the spiral wave tip was not trapped. Above a certain critical value of the heterogeneity strength, however, the spiral wave

tip was intermittently trapped. In the particle model, however, further increasing the depth of the potential well eventually resulted in permanent trapping. This is in contrast to the full model where further increasing the parameter that determines the excitability did not always result in permanent trapping. This can be explained by realizing that the effect of increasing the parameter τ_d has an upper bound, after which further increases do not affect the behavior. In the particle model, however, one can increase the potential well depth indefinitely, which will always result in eventual permanent trapping.

The intermittent trapping was achieved using a circular heterogeneity. In future work, it would be interesting to investigate the effect of the shape of the heterogeneity. In particular, it would be insightful to examine how the curvature of the defect affects the trapping of the spiral wave. Additional future work can address how electric fields used, for example, in low-energy defibrillation methods [38,39], affect the intermittency of the spiral waves. Previous studies have shown that these fields can generate zones of depolarization and hyperpolarization close to the heterogeneity, which can unpin an anchored rotating wave [40,41]. It would be interesting to see how these fields will alter the intermittency found in the current paper.

Clinically, AF is a disease that affects mainly older patients and is a progressive disease, with episodes that increase in duration as patients age. In some AF patients, it appears to display intermittent reentry events, as evidenced in mapping studies [29,30]. Aside from trapping to heterogeneities, other mechanisms may be responsible for this intermittency, including abnormal automaticity or triggered activities that can lead to intermittent reentry. Nevertheless, it is tempting to hypothesize that as patients age, heterogeneities become larger and/or more pronounced, possibly resulting in intermittent trapping of spiral waves. Patients with more progressed AF could then have even larger or more severe heterogeneities, resulting in permanent trapping and persistent AF. This could also explain why targeting the location of the reentry events through ablation (i.e., the destruction of tissue) can result in termination of AF or a marked reduction in AF occurrence [42]. These ablations would remove heterogeneities, which in turn can result in elimination of reentry events [43]. Testing this scenario would require high-resolution mapping studies, coupled with techniques that identify tissue heterogeneities.

ACKNOWLEDGMENTS

We gratefully acknowledge the support of NVIDIA Corporation with the donation of the Tesla K40 GPU used for part of this research. This paper was supported by National Institutes of Health No. R01 HL122384, No. R01 HL149134, and No. R01 HL083359.

-
- [1] I. R. Epstein and K. Showalter, *J. Phys. Chem.* **100**, 13132 (1996).
 - [2] A. T. Winfree, *Science* **175**, 634 (1972).
 - [3] S. Jakubith, H. H. Rotermund, W. Engel, A. von Oertzen, and G. Ertl, *Phys. Rev. Lett.* **65**, 3013 (1990).
 - [4] T. Höfer, J. A. Sherratt, and P. K. Maini, *Proc. R. Soc. London B* **259**, 249 (1995).
 - [5] N. Gorelova and J. Bureš, *Dev. Neurobiol.* **14**, 353 (1983).
 - [6] Y. Yu, L. M. Santos, L. A. Mattiace, M. L. Costa, L. C. Ferreira, K. Benabou, A. H. Kim, J. Abrahams, M. V. Bennett, and R. Rozental, *Proc. Natl. Acad. Sci.* **109**, 2585 (2012).
 - [7] A. Karma, *Annu. Rev. Condens. Matter Phys.* **4**, 313 (2013).
 - [8] J. Jalife, *Annu. Rev. Physiol.* **62**, 25 (2000).
 - [9] M. P. Turakhia, J. Shafirin, K. Bognar, J. Trocio, Y. Abdulsattar, D. Wiederkehr, and D. P. Goldman, *PLoS ONE* **13**, e0195088 (2018).

- [10] Y. Miyasaka, M. E. Barnes, K. R. Bailey, S. S. Cha, B. J. Gersh, J. B. Seward, and T. S. Tsang, *J. Am. Coll. Cardiol.* **49**, 986 (2007).
- [11] Y. Tanaka, N. S. Shah, R. Passman, P. Greenland, D. M. Lloyd-Jones, and S. S. Khan, *J. Am. Heart Assoc.* **10**, e020163 (2021).
- [12] F. H. Fenton, E. M. Cherry, H. M. Hastings, and S. J. Evans, *Chaos* **12**, 852 (2002).
- [13] K. E. Daniels and E. Bodenschatz, *Phys. Rev. Lett.* **88**, 034501 (2002).
- [14] C. Beta, A. S. Mikhailov, H. H. Rotermund, and G. Ertl, *Europhys. Lett.* **75**, 868 (2006).
- [15] D. Vidmar and W.-J. Rappel, *Phys. Rev. E* **99**, 012407 (2019).
- [16] J. N. Weiss, Z. Qu, P. S. Chen, S. F. Lin, H. S. Karagueuzian, H. Hayashi, A. Garfinkel, and A. Karma, *Circulation* **112**, 1232 (2005).
- [17] K. S. McDowell, F. Vadakkumpadan, R. Blake, J. Blauer, G. Plank, R. S. MacLeod, and N. A. Trayanova, *J. Electrocardiol.* **45**, 640 (2012).
- [18] L. Yue, J. Xie, and S. Nattel, *Cardiovasc. Res.* **89**, 744 (2011).
- [19] X. Zou, H. Levine, and D. A. Kessler, *Phys. Rev. E* **47**, R800 (1993).
- [20] F. Xie, Z. Qu, and A. Garfinkel, *Phys. Rev. E* **58**, 6355 (1998).
- [21] D. Olmos, *Phys. Rev. E* **81**, 041924 (2010).
- [22] C. W. Zemlin and A. M. Pertsov, *Phys. Rev. Lett.* **109**, 038303 (2012).
- [23] V. Zykov, A. Krekhov, and E. Bodenschatz, *Proc. Natl. Acad. Sci.* **114**, 1281 (2017).
- [24] A. Defauw, P. Dawyndt, and A. V. Panfilov, *Phys. Rev. E* **88**, 062703 (2013).
- [25] N. Vandersickel, M. Watanabe, Q. Tao, J. Fostier, K. Zeppenfeld, and A. V. Panfilov, *PLoS Comput. Biol.* **14**, e1006637 (2018).
- [26] Z. Y. Lim, B. Maskara, F. Aguel, R. Emokpae, and L. Tung, *Circulation* **114**, 2113 (2006).
- [27] Y.-H. Kim, F. Xie, M. Yashima, T.-J. Wu, M. Valderrábano, M.-H. Lee, T. Ohara, O. Voroshilovsky, R. N. Doshi, M. C. Fishbein *et al.*, *Circulation* **100**, 1450 (1999).
- [28] S. M. Narayan, D. E. Krummen, M. W. Enyeart, and W.-J. Rappel, *PLoS One* **7**, e46034 (2012).
- [29] M. Haissaguerre, A. J. Shah, H. Cochet, M. Hocini, R. Dubois, I. Efimov, E. Vigmond, O. Bernus, and N. Trayanova, *J. Physiol.* **594**, 2387 (2016).
- [30] C. A. Kowalewski, F. Shenasa, M. Rodrigo, P. Clopton, G. Meckler, M. I. Alhousseini, M. A. Swerdlow, V. Joshi, S. Hossainy, J. A. Zaman *et al.*, *Circ.: Arrhythmia Electrophysiol.* **11**, e005846 (2018).
- [31] F. Fenton and A. Karma, *Chaos* **8**, 20 (1998).
- [32] D. M. Lombardo, F. H. Fenton, S. M. Narayan, and W.-J. Rappel, *PLoS Comput. Biol.* **12**, e1005060 (2016).
- [33] R. Abad, O. Collart, P. Ganesan, A. Rogers, M. I. Alhousseini, M. Rodrigo, S. M. Narayan, and W.-J. Rappel, *PLoS ONE* **16**, e0249873 (2021).
- [34] V. Jacquemet and C. S. Henriquez, *IEEE Trans. Biomed. Eng.* **52**, 1490 (2005).
- [35] A. M. Pertsov, J. M. Davidenko, R. Salomonsz, W. T. Baxter, and J. Jalife, *Circ. Res.* **72**, 631 (1993).
- [36] D. M. Lombardo and W.-J. Rappel, *Phys. Rev. E* **99**, 062409 (2019).
- [37] T. Ikeda, M. Yashima, T. Uchida, D. Hough, M. C. Fishbein, W. J. Mandel, P.-S. Chen, and H. S. Karagueuzian, *Circ. Res.* **81**, 753 (1997).
- [38] F. H. Fenton, S. Luther, E. M. Cherry, N. F. Otani, V. Krinsky, A. Pumir, E. Bodenschatz, and R. F. Gilmour Jr., *Circulation* **120**, 467 (2009).
- [39] S. Luther, F. H. Fenton, B. G. Kornreich, A. Squires, P. Bittihn, D. Hornung, M. Zabel, J. Flanders, A. Gladuli, L. Campoy *et al.*, *Nature (London)* **475**, 235 (2011).
- [40] A. Pumir and V. Krinsky, *J. Theor. Biol.* **199**, 311 (1999).
- [41] S. Takagi, A. Pumir, D. Pazo, I. Efimov, V. Nikolski, and V. Krinsky, *Phys. Rev. Lett.* **93**, 058101 (2004).
- [42] S. M. Narayan, D. E. Krummen, K. Shivkumar, P. Clopton, W.-J. Rappel, and J. M. Miller, *J. Am. Coll. Cardiol.* **60**, 628 (2012).
- [43] W.-J. Rappel, J. A. Zaman, and S. M. Narayan, *Circ. Arrhythm. Electrophysiol.* **8**, 1325 (2015).